Tropical cyclone predictability shaped by western Pacific subtropical high: integration of trans-basin sea surface temperature effects

Chao Wang[1,2] · Bin Wang[1,2]

Abstract

Sea surface temperature (SST) anomalies in the Pacific, Indian and Atlantic oceans were suggested to explain inter-annual variability of tropical cyclone (TC) activity over the western North Pacific (WNP). Here we show that the influences of these "trans-basin" SST anomalies in the three oceans can be collectively understood via two leading modes of variability of WNP subtropical high (WNPSH). The first mode, which is forced by SST anomalies in the eastern-central Pacific and tropical Atlantic, can shift TC formation locations southeastward/northwestward, but has insignificant influence on the total TC genesis number, albeit affects the TC tracks, total number of tropical storm days, and power dissipation index (PDI). The second mode, which is a coupled ocean–atmosphere mode associated with a dipole SST anomaly in the Indo-Pacific warm pool, has a significant control on the total TC genesis number. A set of physics-based empirical models is built to predict the two WNPSH modes and TC activity (genesis number, tropical storm days and PDI) in the peak TC season (July–September) with preceding season trans-basin SST predictors. The predictions capture very well the inter-annual variabilities of the WNPSH and reasonably well the variability of WNP TC activity. These results thus establish a unified framework to understand and forecast the inter-annual variability in TC activity over the WNP.

Keywords Western North Pacific · Subtropical high · Tropical cyclone · Seasonal prediction · Inter-annual variability

1 Introduction

Billions of people in Pacific islands and coastal regions are frequently subject to TC-induced damages including gale winds, heavy precipitation, storm surges and landslides (Zhang et al. 2009). Extensive research works have been carried out to understand variations in TC activity over the WNP which experiences considerable inter-annual variability (Chan and Shi 1996; Chia and Ropelewski 2002; Chan 2005; Chen et al. 2006). Numerous studies suggested that such inter-annual variability is closely related to the El Niño–Southern Oscillation (ENSO) phenomenon (Chan 1985, 2000; Lander 1993, 1994; Wang and Chan 2002; Camargo and Sobel 2005; Camargo et al. 2007b; Zhao et al. 2010; Kim et al. 2011; Wang et al. 2013b, 2018a, b; Wang and Wu 2016). In summary, the warm phase of ENSO, namely, El Niño, can shift TC formation locations southeastward by eastward migrating the low-level monsoon trough and tropical upper troposphere trough (TUTT), and intensify TCs through prolonging their lifespans over the warm ocean. The opposite is true for La Niña events. However, it is found that ENSO has little effect on the total TC genesis number over the WNP in the peak season (Lander 1993; Wang and Chan 2002).

Due to the weak relationship between the total TC genesis frequency and local SST variations over the WNP, recently, some studies tried to seek for sources of inter-annual variability outside of the WNP basin. For example, Zhan et al. (2011) suggested that SST anomalies over the eastern Indian ocean can influence the WNP TC genesis number by exciting

✉ Bin Wang
 wangbin@hawaii.edu

 Chao Wang
 wangchao@nuist.edu.cn

[1] Key Laboratory of Meteorological Disaster of Ministry of Education, Joint International Research Laboratory of Climate and Environment Change, Collaborative Innovation Center on Forecast and Evaluation of Meteorological Disasters and Pacific Typhoon Research Center, Nanjing University of Information Science and Technology, Nanjing, China

[2] Department of Atmospheric Sciences and International Pacific Research Center, University of Hawaii at Manoa, Honolulu, HI 96822, USA

equatorial Kelvin waves propagating into the WNP that can lead to anomalous anti-cyclonic/cyclonic circulations over the WNP. Meanwhile, Du et al. (2011) examined the impacts of the delayed Indian ocean warming after strong El Nino events on TC genesis. More recently, the impact of Atlantic SST on the WNP TC genesis frequency has been proposed (Huo et al. 2015; Yu et al. 2015; Zhang et al. 2017, 2018). These studies suggested that Atlantic SST anomalies can induce SST anomalies in the eastern Pacific (Ham et al. 2013; Huo et al. 2015) or the Indian ocean (Yu et al. 2015), thereby further changing large-scale circulations over the WNP and leading to the anomalous TC genesis. Moreover, the Pacific Meridional mode (PMM) is found to be tightly linked to the TC genesis frequency over the WNP, which exerts its influence through modifying vertical shear and vorticity (Zhang et al. 2016a; Zhan et al. 2017; Wu et al. 2018; Wang et al. 2018b).

Although these remote SST anomalies can account for a portion of the inter-annual variability in TC genesis frequency, it is, essentially, the local large-scale circulation change that modulates the TC activity over the WNP. For instance, an anomalous anti-cyclonic/cyclonic circulation over the WNP is usually used to interpret the role of remote SST forcing in influencing TC genesis frequency (Zhan et al. 2011; Du et al. 2011; Tao et al. 2012; Huo et al. 2015; Yu et al. 2015; Zhang et al. 2016a). Therefore, understanding

the effects of local large-scale circulations on TC activity over the WNP is of essential importance in the first place.

Over the WNP, large-scale circulations regulating TC activity include the WNPSH, the low-level monsoon trough, a northeast-southwest tilted convergence zone extending from the northern Indochina Peninsula to the Philippine Sea, the upper-level South Asia High, and the TUTT over the central North Pacific (Fig. 1, Wu et al. 2015; Wang and Wu 2016, 2018a, b). The configuration of these circulations generally determinates the region of favourable large-scale environments, and thus generally determinates mean development area of TC (Fig. 1, Wang and Wu 2018a, b). However, the monsoon trough and TUTT can only shift the TC formation locations on the inter-annual and inter-decadal time scales (Chen et al. 1998; Chia and Ropelewski 2002; Matsuura et al. 2003; Wu et al. 2012, 2015; Wang and Wu 2016, 2018a, b; Huangfu et al. 2017). On the other hand, the WNPSH, which is usually accompanied by large-scale descending motion, low humidity and low-level anti-cyclonic vorticity, is thought to be most closely related to the total TC genesis frequency over the WNP (Liu and Chan 2013). Recently, considerable inter-annual variability of the WNPSH has been documented (Sui et al. 2007; Park et al. 2010; Chung et al. 2011; Wang et al. 2013a; He and Zhou 2014). Although both modes are characterized by an anomalous anti-cyclonic circulation over the WNP, the
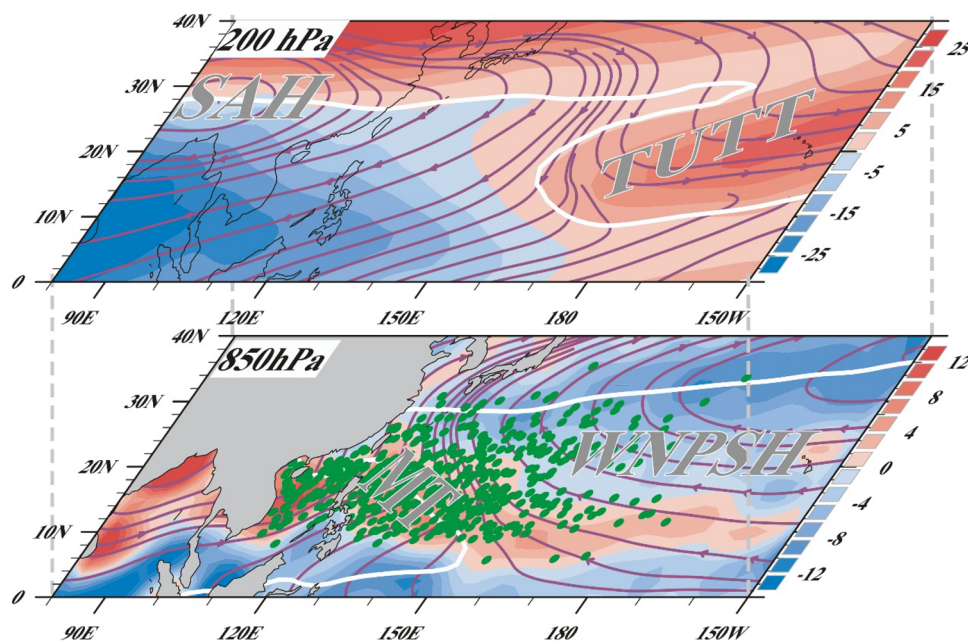
Fig. 1 Large-scale circulations regulating TC activity over the WNP. The upper level shows the July–September mean 200 hPa streamlines and vertical shear of zonal wind (the difference between 200 hPa and 850 hPa zonal wind, shadings, m s⁻¹) during 1981–2010. The lower level shows the July–September mean 850 hPa winds (streamline) and relative vorticity (shadings, 10–6 s⁻¹) during 1981–2010. TUTT represents the tropical upper tropospheric trough, SAH represents the south Asia high, MT represents the monsoon trough, and the WNPSH represents the western North Pacific subtropical high. The green dots denote the corresponding TC formation locations, and the thick white lines show the zero contours of zonal wind speed

underlying physical mechanisms are quite different. Wang et al. (2013a) has shown that the first mode of WNPSH variability is a coupled atmosphere–ocean mode maintained by a positive thermodynamic feedback between the WNPSH and underlying dipole SST anomalies (SSTA) across the northern Indian ocean and WNP, while the second mode is a forced mode that is related to the SST anomalies over the equatorial central Pacific as well as the convection over the maritime continent. Therefore, investigation of the impact of these two modes on TC activity is advantageous to enrich our understanding about the mechanism of TC variability over the WNP.

Thorough understanding the variability and predictability of TC activity makes it possible to obtain skilful seasonal forecast products for TC activity. Over the WNP, the operational seasonal forecast of TC activity becomes available since the early 1990s (Zhan et al. 2012). Various schemes, including statistical methods, dynamical models, and so-called hybrid statistical–dynamical approaches, have been proposed to make seasonal forecasting of the TC activity over the WNP (Camargo et al. 2007a; Zhan et al. 2012). Although the skill of coupled dynamic models in directly predicting TC activity has been improved continuously over the past decades (Chen and Lin 2013; Vecchi et al. 2014; Camp et al. 2015; Manganello et al. 2016), some statistical approaches, which are built upon the identification of the appropriate predictors, show significant forecasting skill and are still the dominant seasonal forecasting strategies for the TC activity over the WNP (Chan et al. 1998, 2001; Camargo et al. 2007a; Fan and Wang 2009; Lu et al. 2010; Zhan and Wang 2016; Kim et al. 2017; Zhang et al. 2016b; Zhan et al. 2012). However, the biases in the current statistical forecasting products have remarkably increased in recent years (Zhan et al. 2012), suggesting the unstable statistical relationships between the TC activity and predictors.

Recently, Wang et al. (2013a) proposed a strategy to build PEMs based on understanding of the physical processes linking the predictors and predictand, to predict the WNPSH and TC activity. In this strategy, only physically meaningful predictors are selected, which is different from the traditional statistical model, and it shows better predicting skill comparing to that of the purely statistical models (Wang et al. 2013a, 2015). Considering the large prediction biases in traditional statistical models over the WNP (Zhan et al. 2012) and the high predictability of the WNPSH (Wang et al. 2013a), the PEM provides an alternative way to predicting TC activity if we can establish the physical connection between the WNPSH and TC activity.

However, previous studies mainly focused on the effects of WNPSH on TC prevailing tracks (Ho et al. 2004; Wu et al. 2005; Liu and Chan 2008), its effect on TC formation has not been explicitly documented. Therefore, the primary objectives of this study are to reveal the effects of WNPSH on the WNP TC activity in terms of its two major modes of inter-annual variability, and to establish a set of PEMs to predict TC activity by taking advantage of the high predictability of the WNPSH. In this work, we will demonstrate that the variations in the WNPSH may reflect the integrated influences of the SST anomalies in the tropical Pacific, Indian and Atlantic (trans-basin SST anomalies for short) on TC activity over the WNP. This will establish a uniform framework to understand and forecast the inter-annual variability in the WNP TC activity.

Section 2 describes the data and method. Section 3 introduces the two inter-annual modes of WNPSH and the related trans-basin SST variability. The impacts of the two subtropical high modes on TC activity and the corresponding large-scale conditions are illustrated in Sect. 4. Section 5 further presents the high predictability of WNPSH and its application to seasonal forecasting of WNP TC activity, followed by a summary in Sect. 6.

2 Data and method

Best track data from the Joint Typhoon Warming Center (JTWC), the Japan Meteorological Agency (JMA) and the Chinese Meteorology Administration (CMA) are used to obtain TC information. TCs in this study are defined as tropical storms whose maximum wind speed reach or exceeds 17.2 m s^{-1}. As the results derived from the JTWC, CMA and JMA data are generally similar, only the findings based on the JTWC best track data are presented. The monthly atmospheric data are obtained from the National Centers for Environmental Prediction (NCEP)-National Center for Atmospheric Research (NCAR) reanalysis (Kalnay et al. 1996). The monthly SST from Extended Reconstruction SST (ERSST) version 4 (Huang et al. 2015) is used to document the SST anomalies related to inter-annual variability of WNPSH.

The analysis period is from 1965 to 2016, and we focus on the peak season (July–September, JAS) of TC activity over the WNP (0°–40°N, 100°E–180°). 1965 is taken as the starting year because satellite monitoring became routine around this year (Wang and Chan 2002; Chan 2006). An 8-year high-pass Fourier filter is first applied to all observational data to isolate interannual variability. Because the conventional definition of subtropical high by using geopotential height cannot eliminate the effects of global warming-induced pressure rising (Wu and Wang 2015), we use 850 hPa wind field to perform multivariate Empirical Orthogonal Function (EOF) analysis (Wang 1992) to obtain the dominant modes of atmospheric circulation (Park et al. 2010; He and Zhou 2014). Composite and correlation analyses are also employed to present the results and statistical

significance is assessed using the two-tailed Student's t-test (Wilks 2006).

The PEMs are derived by multivariate regression (Wang et al. 2013a). All variables are standardized before regression, which allows us to infer the relative contribution of each predictor by examining the normalized regression coefficient. Two validation methods, including leave-three-out cross-validated reforecast and independent forecast, are used to verify the prediction skills of PEMs (Wang et al. 2015; Li and Wang 2017; Luo and Wang 2017). The cross-validated reforecast is conducted by training the PEMs with the samples leaving 3 years out each time, and then apply the derived PEMs to predict the predictands in three withheld years (Michaelsen 1987). The training process is repeated for all the other years to get the cross-validated reforecast for 1965–2000. The independent forecast is then performed for the rest 16-year (2001–2016). The temporal correlation coefficient (TCC) and Mean Square Skill Score (MSSS) are used to measure the deterministic seasonal forecast skill (Murphy 1988). The MSSS compares the Mean Square Error (MSE) of forecast to the MSE of climatology and thus reflect the forecast skill relative to the "forecasts" of climatology. The MSSS is defined as,

$$MSSS = 1 - \frac{MSE}{MSE_c},$$

The MSE is defined as $MSE = \frac{1}{n}\sum_{i=1}^{n}(f_i - x_i)^2$, which is the MSE of the forecast. The MSEc, the MSE of climatology, is given as $MSEc = \frac{1}{n}\sum_{i=1}^{n}(x_i - \bar{x})^2$, where n, x_i, f_i, and $\bar{x}$ represent the time steps of forecasting, observation in each step, forecasted value in each step and climatological mean of observation, respectively.

3 Two dominant modes of inter-annual variability of the WNPSH

Figure 2 shows the two leading EOF modes of 850 hPa winds over the WNP. The first (second) mode can explain 44.8% (16.6%) of the total variance. Both modes feature an anomalous anti-cyclonic circulation over the WNP. The first mode shows an anti-cyclonic circulation anomaly occupying the entire WNP with two centers located at (18°N, 150°E) and the northernmost South China Sea, respectively (Fig. 2a). The anomalous easterly in the southern flank of the anti-cyclonic circulation is located over the tropical WNP, which is different from that in the second mode (Fig. 2b). The anti-cyclonic circulation of the second mode is slightly shifted northward with a center at (25°N, 140°E), and an anomalous cyclonic circulation occurs over tropical southeast WNP.

The first model is thought to be related with SST variation over the equatorial central Pacific and the convection over

the maritime continent, the second mode is a coupled mode maintained by a positive air-sea thermodynamic feedback (Wang et al. 2013a). Since the EOFs derived from 850 hPa winds are different from those derived from the geopotential height, and the seasons (JJA vs. JAS) are also slightly different, we need to re-examine the origins of the two modes.

Figure 3 shows the regressed SST anomalies with respect to the principal components of the two modes. The first mode concurs with an equatorial dipole SST anomaly with a cooling in the equatorial central-eastern Pacific and a warming over the Marine Continent (Fig. 3a), which resembles that of a La Niña developing phase. The first principal component (PC1) is significantly correlated with the Niño3.4 index with a correlation coefficient of -0.77 (p < 0.01). On the one hand, the SST cooling over the equatorial central Pacific can, through suppressing convective heating, induce a Rossby wave response that can strengthen the WNPSH directly (Wang et al. 2013). On the other hand, the SST warming over the Marine Continent can enhance convective heating, inducing the equatorial easterly anomaly over the WNP as a Kelvin wave response, which further reinforces the WNPSH by generating anticyclonic shear vorticity (Chung et al. 2011; Wang et al. 2013a; Li et al. 2017). Thus, to a large extent, the first mode can be viewed as a forced mode by ENSO. In addition, the strengthened WNPSH coincides with a significant anomalous SST warming over the equatorial Atlantic (Fig. 3a). Previous studies have suggested that the tropical Atlantic warming induced atmospheric heating can intensify easterly trade winds in the off-equatorial eastern Pacific by emanating Rossby waves (Vimont et al. 2001), intensifying trade winds and contributing to the equatorial Pacific cooling through the Bjerknes feedback (Kucharski et al. 2011; Ham et al. 2013; Wang et al. 2013a; McGregor et al. 2014; Li et al. 2015; Kajtar et al. 2017; Zhang et al. 2018). The eastern Pacific cooling can indirectly influence the WNPSH. In other words, the first mode of WNPSH, in fact, integrates the impacts of ENSO over the Pacific and the tropical Atlantic SST anomalies.

To confirm the aforementioned relationship, the time series of the two principal components and the equatorial central-eastern Pacific SST and tropical Atlantic SST are shown in Fig. 4. The equatorial central-eastern Pacific SST are averaged over the (10°S–10°N, 180°E–100°W) and the Atlantic SST anomalies are averaged over (10°S–20°N, 70°W–0°). The correlation coefficient between the PC1 and the equatorial central-eastern Pacific SST and the Atlantic SST anomaly attains values of -0.81 and 0.52, respectively. Note also that, the equatorial central-eastern Pacific SST and the Atlantic SST anomalies are statistically independent of each other (r = -0.17 for 1965–2016), but both have significant correlations with the PC1, which indicates the synergetic effects of Pacific and Atlantic SST anomalies on the first mode of WNPSH (Fig. 4a, b).

Fig. 2 Leading modes of 850 hPa wind over the WNP. **a** The first multivariate EOF mode and **b** the second multivariate EOF mode of July–September mean 850 hPa winds during 1965–2016. The percentage of variance explained by individual modes is shown on the top-right of each panel
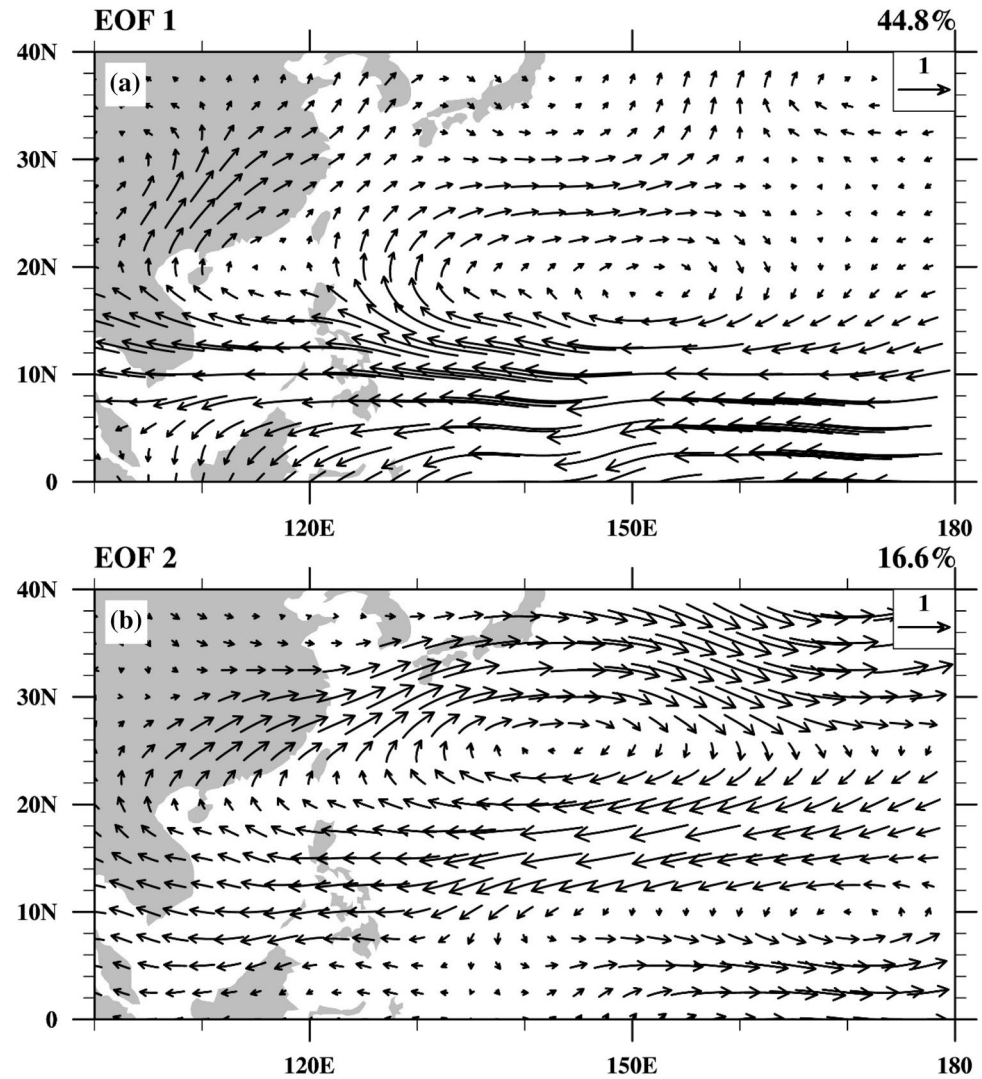
Fig. 3 Variability sources of the two WNPSH modes. Regressed SST anomalies in July–September with respect to the time series of **a** the first and **b** the second EOF modes during 1965–2016. Purple vectors show the two leading modes of 850 hPa winds shown in Fig. 2 and the green lines outline the WNP. Dots denote areas that are significant at the 95% confidence level
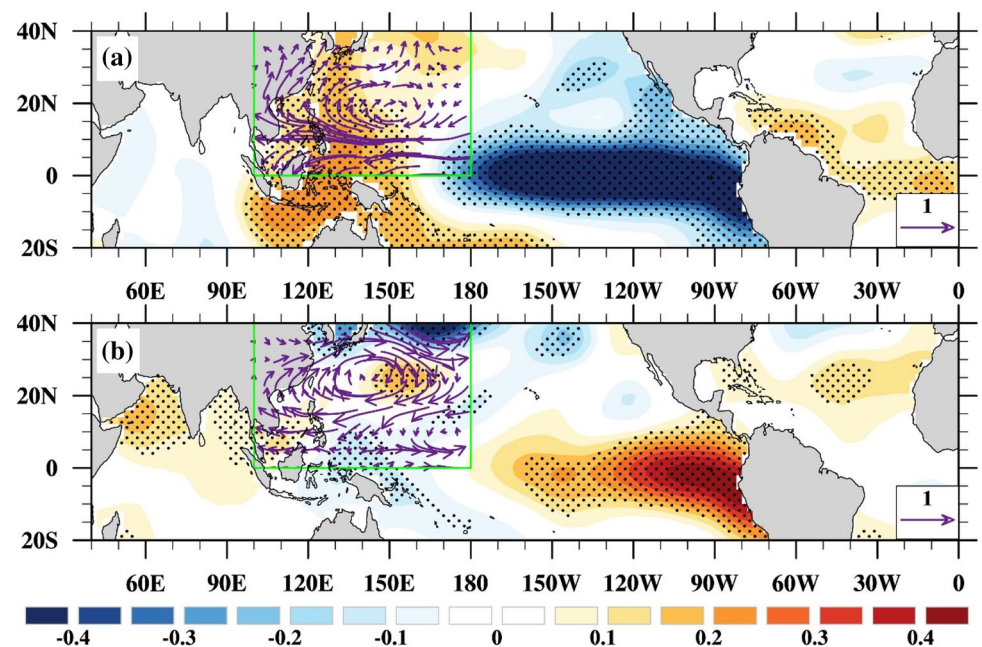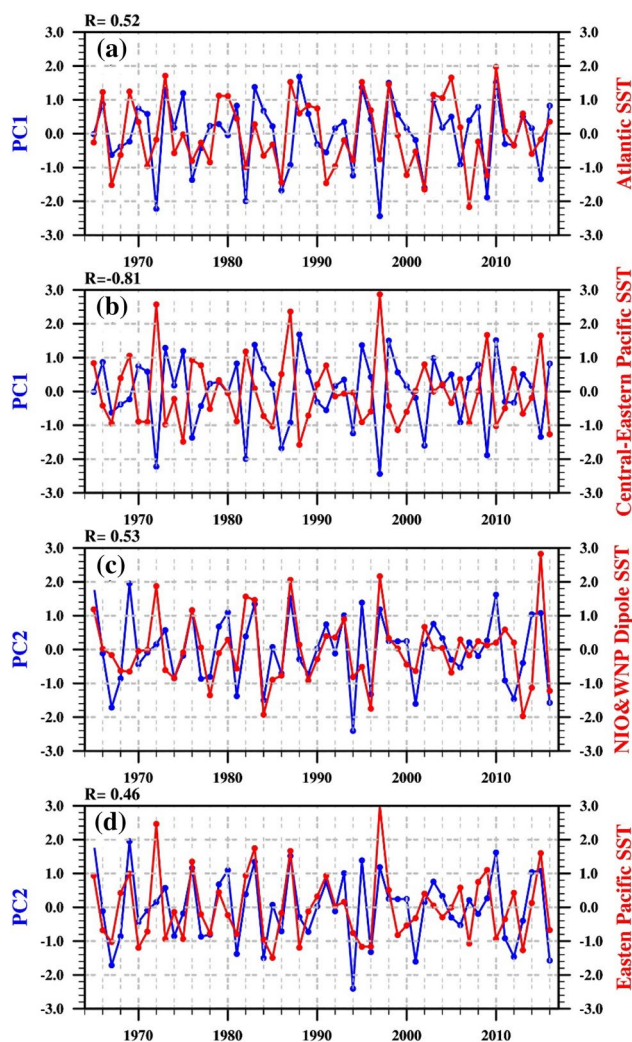
Fig. 4 Relationship between the two WNPSH modes and trans-basin SST variations. Time series of **a** the first principal component and Atlantic SST (10°S–20°N, 70°W–0°), **b** the first principal component and SST over the equatorial central-eastern Pacific (10°S–10°N, 180°E–100°W), **c** the second principal component and dipole SSTA difference between the NIO (0°–25°N, 50°E–110°E) and the WNP (0°–15°N, 130°E–170°E), **d** the second principal component and the SST over the equatorial eastern Pacific (10°S–10°N, 120°W–80°W) in July–September during 1965–2016. The corresponding correlation coefficient R is shown on the top-left of each panel

For the second mode, the regressed SST anomalies are generally weaker than those associated with the first mode (Fig. 3b). Anomalous warming is seen in the northern Indian Ocean and the South China Sea, while weak negative SST anomalies can be found to the southeast flank of WNPSH. Wang et al. (2013a) suggested that the strengthened WNPSH is coupled to the underlying dipole SST pattern in the Indo-Pacific warm pool through a positive thermodynamic feedback. On one hand, the anomalous northeasterly to the east and southeast flank of WNPSH superposed on the mean easterly winds, increases the total wind speed, enhances the

sea surface evaporation, thus cools the SST. On the other hand, the anomalous northeasterly transport dry air to the southeast of the anomalous WNP anticyclone. Both the SST cooling and dry advection reduce convective instability and suppress convection to the east and southeast of the anticyclone. The reduced convective heating can then generate descending Rossby waves, which serves to reinforce the WNPSH. The atmosphere–ocean feedback mechanism is supported by numerical experiments with coupled climate models (Lau and Nath 2003; Lau et al. 2004; Wang et al. 2013a; Xiang et al. 2013). This feedback mechanism is thought to be strong during spring and early summer and gradually weakening toward late summer because the cooling to the east weakens. Note, however, Xiang et al. (2013) demonstrated that during the late summer the atmospheric Rossby response can be significant even to a weak SST anomaly (0.2–0.3 °C) in the WNP because the background SST is over 29 °C and mean precipitation is enhanced. In addition, the dry advection and atmospheric stabilization to the southeast of the anticyclone remain in action in late summer. For the Indian Ocean sector, on one hand, the anomalous WNPSH forcing can lead to the SST warming through reducing cloudiness and surface evaporation cooling (Du et al. 2009); On the other hand, the warming can stimulate a warm atmospheric Kelvin wave response, generate anticyclonic shear vorticity and suppress convection over the WNP that further enhance the WNPSH (Yang et al. 2007; Xie et al. 2009; Wu et al. 2009). More recently, the atmosphere–ocean thermodynamic feedback mechanism maintaining the WNPSH is generally considered as a coupled ocean–atmosphere mode across the Indo-Pacific warm pool (Wang et al. 2013a, 2017; Xie et al. 2016; Li et al. 2017). That is, the second mode can be viewed as an atmosphere–ocean interaction mode combining the effects of northern Indian Ocean and WNP SST anomalies. The above assertion can be further confirmed by investigating the second principal component (PC2) and the dipole SSTA difference between the NIO (0°–25°N, 50°E–110°E) and the tropical eastern WNP (0°–15°N, 130°E–170°E) over the 1965–2016 (Fig. 4c). Indeed, they are significantly correlated with a correlation coefficient of 0.53 (p < 0.01).

Additionally, a warming signal can be found in the equatorial eastern Pacific (Fig. 3b). The warming over the equatorial eastern Pacific can favor formation and maintenance of the WNPSH by setting up a lower tropospheric teleconnection pattern. Initially, the enhanced convective heating associated with the eastern Pacific warming can stimulate an anomalous cyclone north of the equator in the central Pacific as a Rossby wave response. The northeasterly to the western flank of the anomalous cyclone can transport dry air and cools SST in the WNP, which in turn, enhances the atmosphere–ocean thermodynamic feedback associated with the WNPSH. Therefore, the SST anomaly over

the equatorial eastern Pacific (10°S–10°N, 120°W–70°W) is closely related with the NIO-WNP dipole SSTA (r = 0.74, p < 0.01). Although the eastern Pacific warming is significantly correlated with the PC2 (Fig. 4d, r = 0.46, p < 0.01), it is not an independent factor as it is highly correlated with the NIO-WNP dipole SSTA. It should be noted that the dipole SSTA differs from the relative SST proposed by Vecchi and Soden (2007). The concept of relative SST proposed by Vecchi and Soden (2007) is to emphasize the importance of spatial pattern of SST changes on the tropical cyclone potential intensity, while the motivation of using the dipole SSTA in this study is to quantify the atmospheric dynamic response to the SST changes in the Atlantic and Indian ocean basins, and the effects of trans-basin SST variation on the western North Pacific subtropical high.

The two modes of WNPSH can reflect very well the influences of SST variations in the tropical Pacific, Indian Ocean and tropical Atlantic, which are usually identified as the potential sources of inter-annual variability in the WNP TC activity. Therefore, investigating the impacts of these two WNPSH modes on local TC activity can help us to establish a uniform framework to understand the connections between the trans-basin SST variability and the TC activity over the WNP.

4 Control of the WNPSH dynamics on WNP TC activity

Distinct circulation patterns of the two modes and the related driving mechanisms signify their possible different impacts on TC activity. Here composite analysis for the two modes is conducted to verify this hypothesis. The composite years are selected according to the criteria that the anomalous PC exceeds one standard deviation. Accordingly, seven strong positive cases (1973, 1975, 1983, 1988, 1998 and 2010) and nine strong negative cases (1972, 1976, 1982, 1986, 1994, 1997, 2002, 2009 and 2015) are chosen for the first mode. Obviously, these years are related to developing ENSO event, confirming the PC1 is a forced mode. Meanwhile, 12 strong positive cases (1965, 1969, 1976, 1980, 1983, 1987, 1993, 1995, 1997, 2010, 2014 and 2015) and eight strong negative cases (1967, 1981, 1984, 1994, 1996, 2001, 2012, and 2016) are selected for the second mode. Note that we

Fig. 5 Influences of the two WNPSH modes on TC formation distribution. **a** Climatology (contours, counts) over 1981–2010 and the composite TC genesis frequency anomalies (shadings, counts decade-1) in July–September between the positive and negative phase of the first mode of WNP winds. **b** the same as in **a** except for the second mode. Dots denote areas that are significant at the 90% confidence level
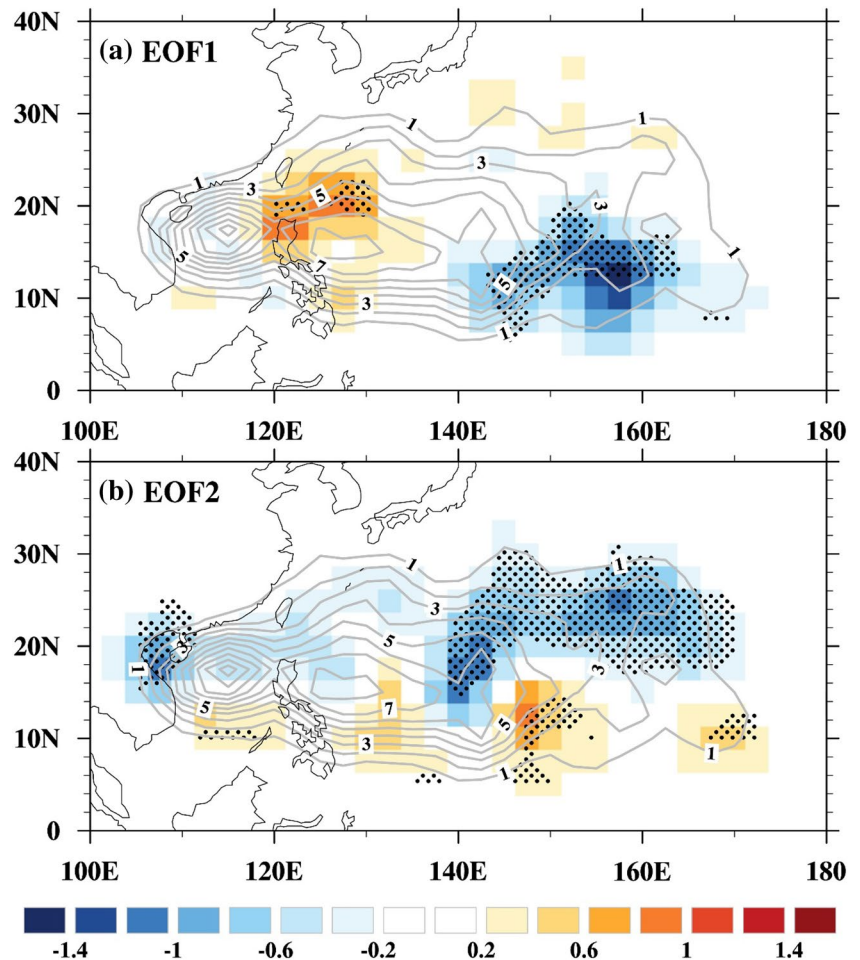
have argued that the second mode is the coupled WNPSH and dipole SST mode. Various physical interpretations were proposed to explain the anomalous strong WNPSH that usually occurs during El Niño decaying summer, including atmosphere–ocean interaction theory (Wang et al. 2000, 2003, 2013a, 2017; Li et al. 2017), Indian Ocean capacitor theory (Yang et al. 2007; Xie et al. 2009, 2016) and combination mode theory (Stuecker et al. 2013, 2015). While the atmosphere–ocean interaction theory can make the WNPSH sustained by itself, both the latter two theories highly depend on the El Niño forcing. However, about one-half of the positive years for the second mode do not concur with decaying

El Niños, indicating that the second mode can be independent of El Niño decay. Thus, the atmosphere–ocean interaction theory provides a more comprehensive framework to understand the inter-annual variation of the WNPSH in both El Niño and non-El Niño years.

4.1 Impacts on the TC formation, track, and intensity

The influences of the two modes on the TC activity display distinct features in terms of the spatial distribution of TC genesis (Fig. 5). The composite results for the first mode
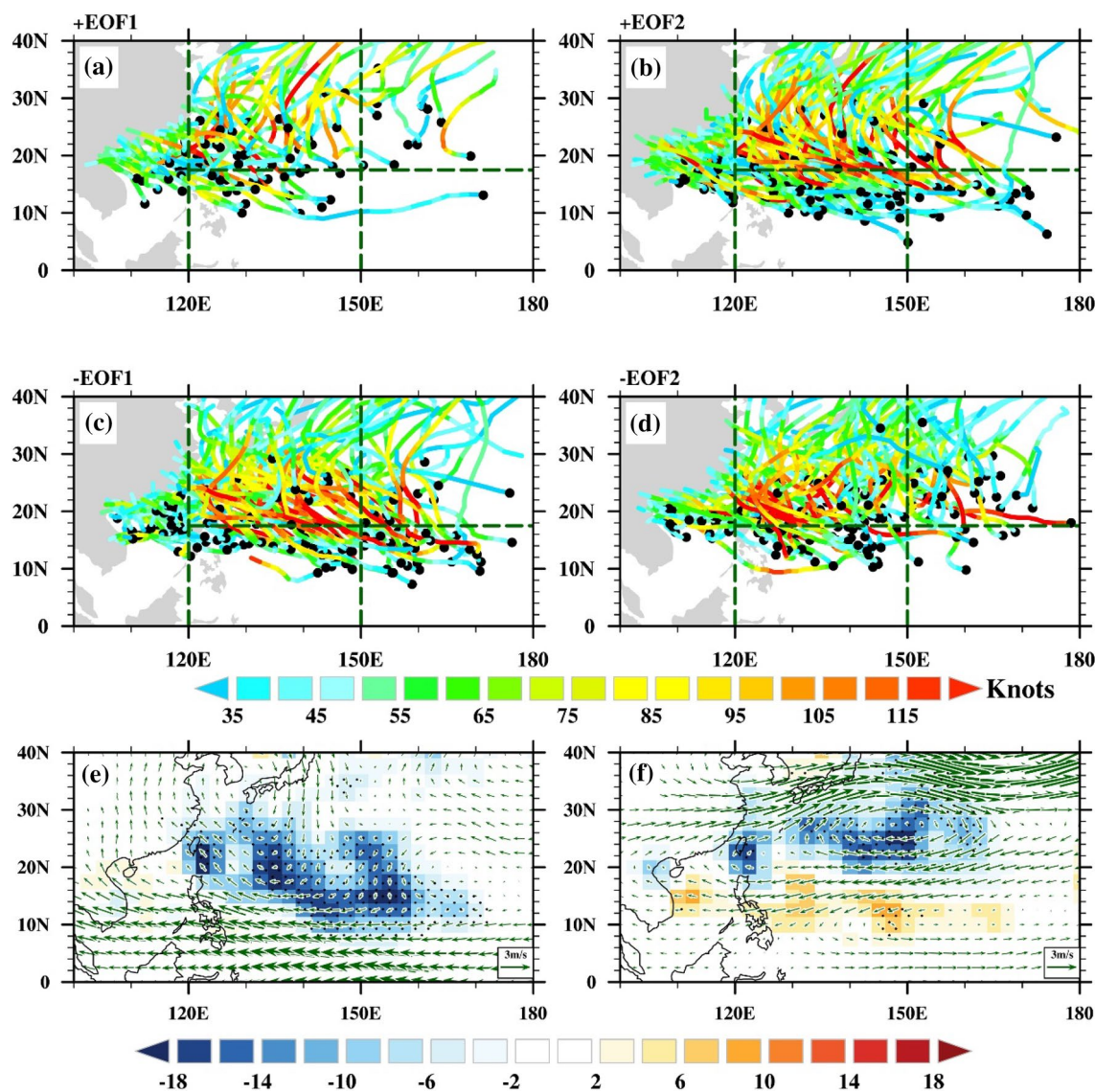
Fig. 6 Influences of the two WNPSH modes on TC track and intensity. TC tracks and intensity (color shading, knots) in July–September during **a** the positive and **c** negative phase of EOF1. **b, d** The same as **a** and **c**, respectively, but for the second mode. Composite TC track density anomalies at each 2.5° latitude × 2.5° longitude box (occurrences decade-1) and steering flow anomalies (vectors, m s^{-1}) between the positive and negative phase of **e** the first mode and **f** the second mode. Dots in **e** and **f** denote areas that the density differences are significant at the 90% confidence level

feature increased TC formation number in the northwest quadrant and suppressed TC formation in southeast quadrant over the WNP. The dipole distribution resembles the results based on strong ENSO composites (Wang and Chan 2002; Camargo et al. 2007b; Wang and Wu 2016). For the second mode, the composite TC formation displays two zonally elongated anomalies separated by 15°N. To the north of 15°N, negative anomalies prevail with the minimum positive center located mainly over the northeastern quadrant of the WNP. To the south of 15°N prevail positive anomalies with the maximum centered on the region over the southeastern quadrant of the WNP (Fig. 7b). Such a distribution generally agrees with Zhan et al. (2011), in which Indian ocean SST anomalies is significantly negatively correlated with the WNP TC genesis frequency.

Figure 6 further shows the TC track and intensity in the positive and negative phases of the two modes and their corresponding differences (Fig. 6e, f). During the positive phases of the first mode, the effects of suppressed TC formation in the southeastern WNP and enhanced eastward steering flow overwhelms the effect of increasing TC formation in the northwest WNP, leading to suppressed TCs activity east of 120°E (Figs. 5a, 6e). On the other hand, for the second mode, the track density anomalies are featured with growing number of TCs influencing the region south of 17.5°N and less TC entering subtropical region during the positive phase, which is consistent with the anomalous

TC formation distribution and the zonally dominated anticyclonic steering flow anomalies (Figs. 5b, 6f). The TC intensity can be indicated by its residence time over the tropical warm ocean (Wang and Chan 2002; Camargo and Sobel 2005; Wing et al. 2007; Zhao et al. 2011; Wang and Wu 2012, 2015). In particular, the TC formation locations shift northwestward and their tracks are much shortened in the positive phase of PC1, which reduces the time for TC staying on the warm ocean, and thus TCs are weaker than those during the corresponding negative phases (Fig. 6a, c). Again, TCs formed during positive phases of PC2 can attain stronger intensity than those in negative phases due to the equatorward shift of TC formation locations and prolonged path (Fig. 6b, d).

Concerning the TC genesis number, both the WNPSH modes tend to suppress TC formation over the WNP. On average, 12.2 TCs formed over the WNP in positive phases and 13.6 TCs formed in negative phases of the first mode. For the second mode, 13.3 TCs formed over the WNP during positive phases and 16.7 TCs formed in negative phases. But only the difference of the second mode is significant at 90% confidence level. Indeed, the distinct effects of the two modes on TC formation can be found in their inter-annual time series as well (Fig. 7). It can be seen that the TC genesis frequency over the WNP has no significant correlation with PC1, but it is significantly correlated with PC2 during 1965–2016 (correlation coefficient r = − 0.64, p < 0.01). It

Fig. 7 Relationship between the two WNPSH modes and TC genesis number over the WNP. Time series of the normalized WNP TC genesis number (red) along with **a** PC1 (blue), and **b** PC2 (blue) in July–September during 1965–2016. The correlation coefficient R is shown on the top-left of each panel
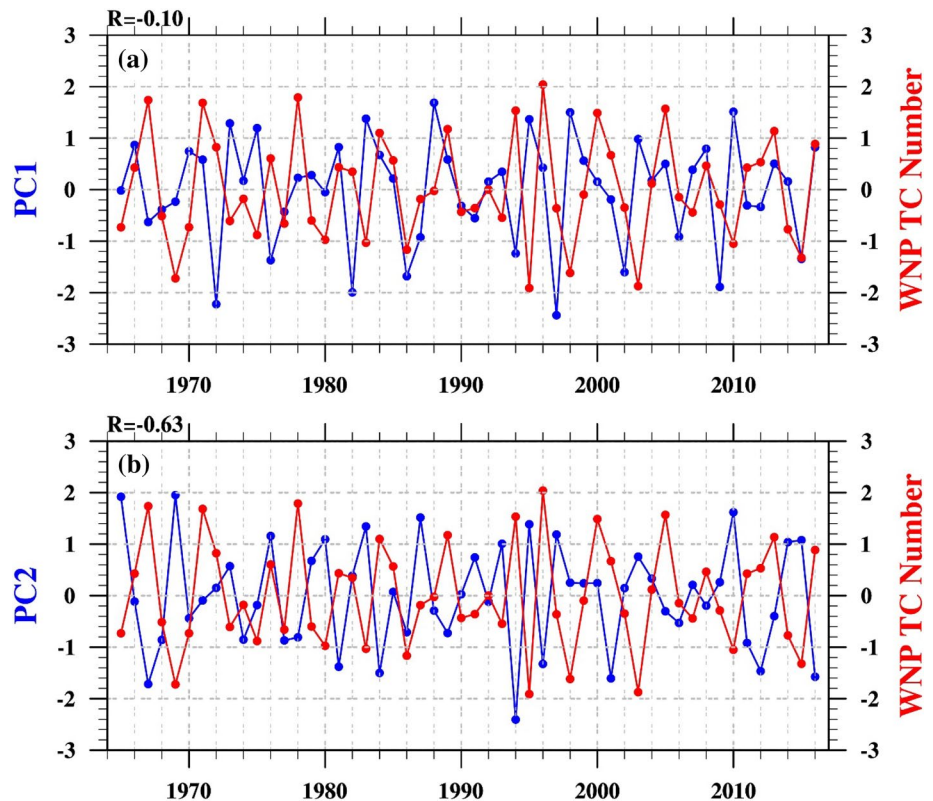
is found that the PC2 is also significantly correlated with the PMM (r = − 0.33, p < 0.05), which was identified as an important factor modifying WNP TC activity (Zhang et al. 2016a). Actually, both the PMM and PC2 are maintained through atmosphere–ocean interaction (Wang et al. 2000; Chiang and Vimont 2004). More recently, some studies found that the positive PMM index in 2016 mainly contribute to the unexpected enhanced WNP TC activity following the strong 2015/2016 El Niño (Zhan et al. 2017; Wu et al. 2018; Wang et al. 2018b). These results indicate the crucial role of SST variations over the subtropical central-eastern North Pacific in the WNP TC activity.

4.2 Influences of the large-scale environmental parameters on TC formation

Large-scale parameters have profound impacts on the TC formation (Gray 1968; Emanuel and Nolan 2004; Murakami and Wang 2010). Therefore, investigation the corresponding large-scale conditions may be instrumental for clarifying the distinct impacts of the two modes on TC formation (Fig. 8).

Generally, the overall patterns of anomalous large-scale parameters are consistent with that of TC formation. During the positive phase of EOF1, the anomalous anti-cyclonic vorticity and the increased vertical wind shear over the eastern WNP are in accordance with the suppressed TC formation in the southeastern WNP. Meanwhile, mid-level relative humidity (500 hPa omega) displays a negative (positive) anomaly over the eastern WNP but positive (negative) anomalies over the tropical western WNP and subtropical eastern WNP, which is in line with the TC formation as well. For the second mode, the meridional tri-polar patterns of relative vorticity and vertical motion mainly contribute to the anomalous TC formation. However, the decreased humidity in the tropical WNP and vertical wind shear north of 15°N are inconsistent with the TC formation in these regions.

To demonstrate the integrated effects of these large-scale parameters on TC formation, a genesis potential index (GPI) developed by Emanuel and Nolan (2004) is presented in Fig. 9. Although some discrepancies exist, the anomalous GPI distribution for two WNPSH modes generally reproduced the anomalous TC formation pattern. The consistency between the GPI and TC formation suggested that the WNPSH can convey
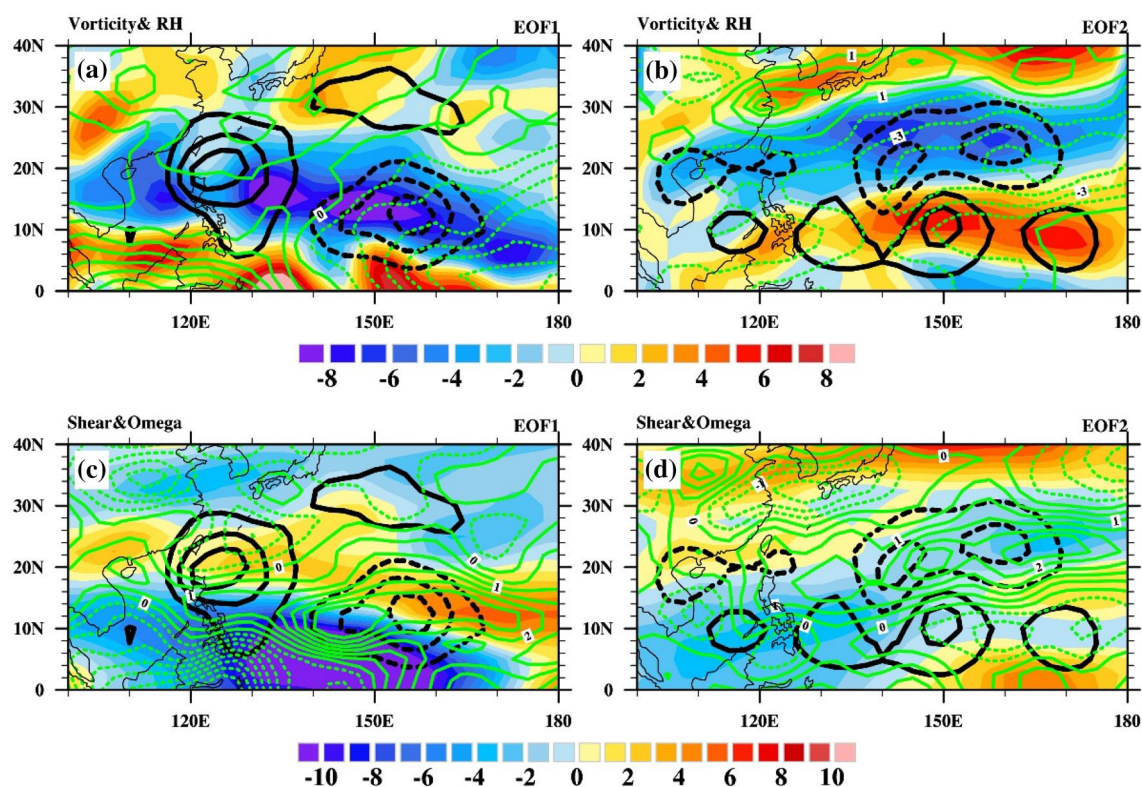
Fig. 8 Influences of the two WNPSH modes on the large-scale environmental parameters. Composite differences between the positive and negative phases of the first mode in **a** 850 hPa relative vorticity (shadings, 10^{-6} s^{-1}) and 600 hPa relative humidity (green contours, %) and **c** vertical wind shear (shadings, m s^{-1}) and 500 hPa omega (green contours, 10^{-2} Pa s^{-1}) in July–September. **b, d** Same as **a, c**, respectively, but for the second mode. The black contours are the corresponding anomalous TC formation shown in Fig. 5. Solid (dotted) contours denote the value greater (less) than zero

its impact on TC formation through modifying the ambient large-scale environments.

5 High predictability of the WNPSH paves a way for seasonal TC forecast

Here we first built PEMs (Wang et al. 2015) to predict the two WPSH modes in the TC peak season with trans-basin SST predictors and linear regressions. Persistent signals defined as the two months mean (May–June) before the forecasting season (July–September), and tendency signals are defined as the difference between May–June mean and previous December–January mean.

For the first mode, two persistent predictors, the SSTA in the central-eastern Pacific and tropical Atlantic are used to construct the PEM for the first mode (Table 1, denoted by CEP and TA, respectively). The correlation coefficient between the May–June mean Pacific and Atlantic SSTA with PC1 are − 0.65 and 0.47, respectively. Physically, the May–June mean SSTA, which in the development phases of an ENSO cycle, can infer the equatorial Pacific SSTA

in the ensuing months by taking advantage of the strong phase-locking property of ENSO (Rasmusson and Carpenter 1982). In addition, the summer Atlantic SST was found can foreshadow the WNPSH variation in the following months, and thus providing an additional source of predictability for the EOF-1. The second mode, which is an atmosphere–ocean interaction mode across the Indo-Pacific warm pool, can be predicted by a precursory dipole SSTA difference between the Indian Ocean and the northwestern Pacific (Table 1, denoted by IOWP). In addition, a tendency predictor for the second mode was identified over North Pacific (Table 1, denoted by NPT), which can favor the WNPSH by transporting dry and cold air and increasing atmospheric stabilization to its southeast. Hence, all these predictors are adopted based on the physical processes that govern the two predictable EOF modes (Wang et al. 2013a).

The PEMs derived using the SST predictors listed in Table 1 can reasonably reproduce the inter-annual variability of two modes of the WNPSH (Fig. 10). The prediction (simulation) temporal correlation coefficient skills for the first and second modes are 0.82 and 0.72, respectively, over

Fig. 9 Influences of the two WNPSH modes on GPI. Composite differences of the GPI in July–September between the positive and negative phase of **a** the first and **b** second mode. Dots denote areas where the differences are significant at the 90% confidence level. The green contours are the corresponding anomalous TC formation shown in Fig. 5. Solid (dotted) contours denote the value greater (less) than zero
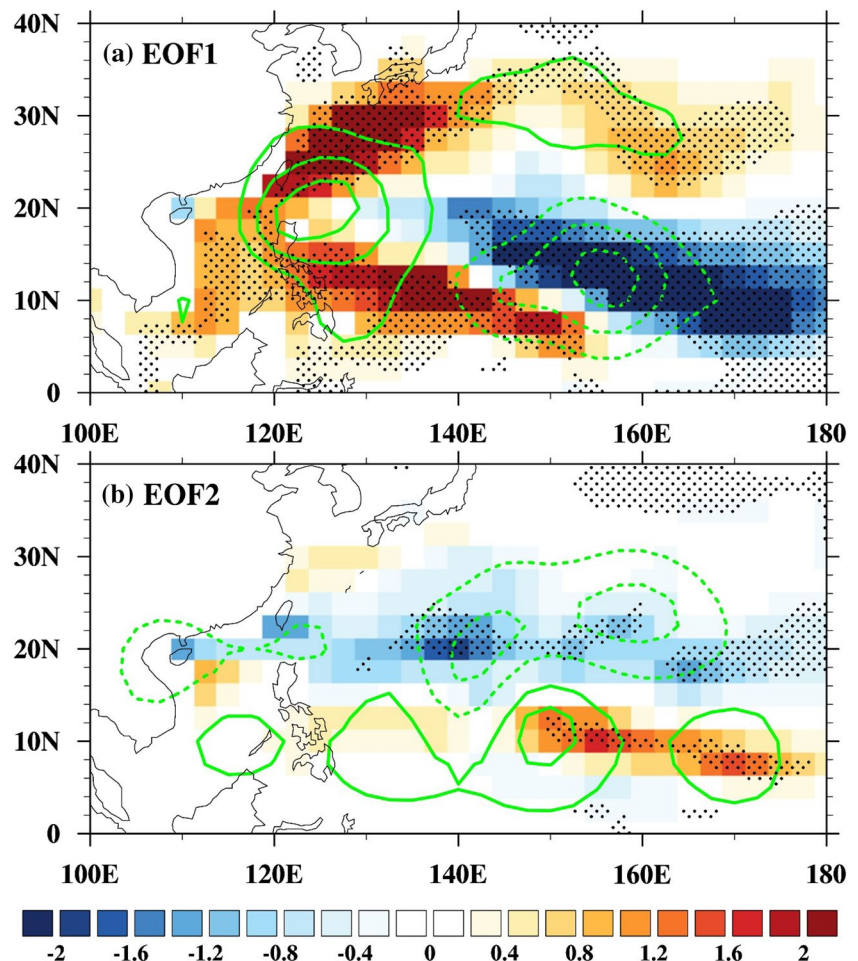
**Table 1** Definitions of the four predictors for WNPSH modes

Name	Definition	Meaning
CEP	May–June SSTA over (10°S–10°N, 180°W–100°W)	Central-eastern Pacific SST predictor
TA	May–June SSTA over (10°S–20°N, 60°W–20°W)	Tropical Atlantic SST predictor
IOWP	May–June SSTA difference between (10°S–25°N, 50°E–110°E) and the (10°–30°N, 130°E–150°W)	Indo-Pacific dipole SST predictor
NPT	May–June minus December–January SST tendency over (45°N–55°N, 150°E–170°W)	North Pacific SST predictor

the 52-year period of 1965–2016. In order to test the skill of the PEM, A leave-three-out cross-validated reforecast is performed by taking 3 years out around the predicted year for 1965–2000. The TCC (MSSS) skills of cross-validated reforecast during 1965–2000 for the first and second modes are 0.79 (0.4) and 0.73 (0.33), respectively, indicating more than 50% of the total variance of these two modes is potentially predictable. To confirm the capacity of the predicting scheme, we used the data of 1965–2000 as training period to derive a prediction equation, and the independent forecast is then made for the rest 16-year during 2001–2016 (Fig. 10). The independent forecast for the first (second) mode has TCC and MSSS skills of 0.83 (0.44) and 0.56 (0.19) for the recent 16 years (2001–2016). The significant TCC of hindcast results indicates the quality skill of the PEMs in predicting the two WNPSH modes.

The high predictability of the two WNPSH modes, in fact, provides a way to predict the TC activity due to the close connection between the WNPSH modes and the WNP TC activity (Figs. 5, 6, 7). Here we attempt to predict the TC activity in peak season (July–September) with zero-month lead (starting from June 30th) by using the two modes of WNPSH as predictors. Namely, we first predict the two modes of WNPSH and then predict the TC activity according to the relationship between the WNPSH modes and TC activity.

Before building the PEMs, we first estimate the potential predictability of TC activity related to WNPSH modes by simulating the TC activity metrics with the observed WNPSH modes in peak TC season (Fig. 11). The TC metrics include basin-wide TC genesis number, tropical storm days and power dissipation index (PDI) over the WNP. The tropical storm days are defined as the total days of 6-h TC records

Fig. 10 Prediction skills of the PEMs for the two WNPSH modes. Time series of **a** PC1, and **b** PC2 obtained from the NCEP reanalysis (black line), cross-validated reforecast (blue line) and prediction (green line). The corresponding TCC and MSSS are shown in the bottom of each panel
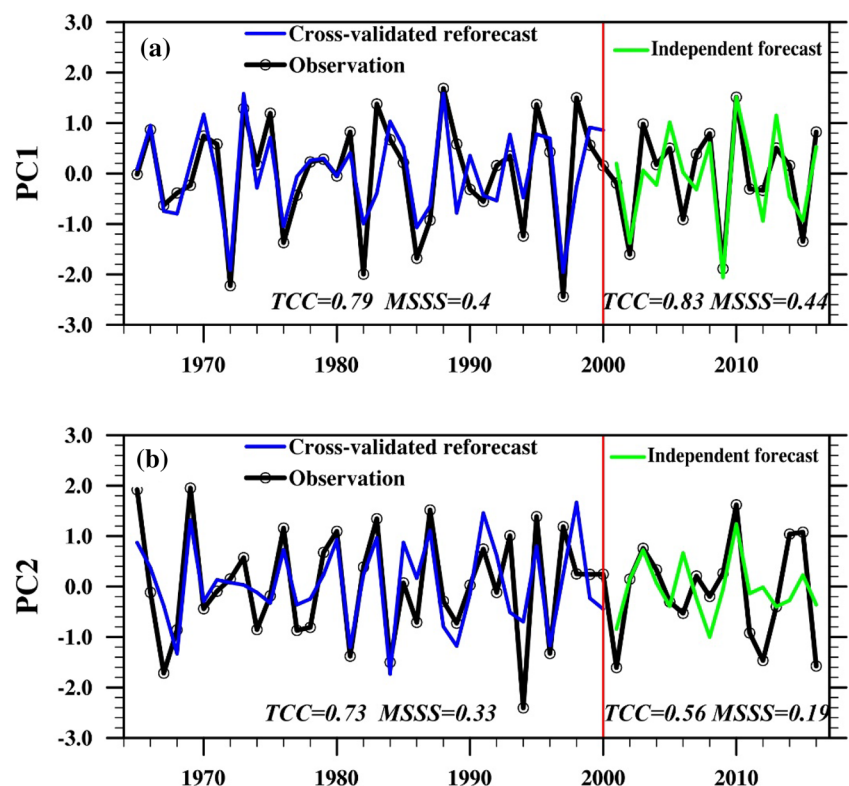
Fig. 11 Predictability of TC activity associated with the two WNPSH modes. Time series of observed (blue line) and simulated (red line) **a** TC number, **b** tropical storm days and PDI with the two observed WNPSH modes in peak TC season. The corresponding correlation coefficient R is shown in the top left of each panel
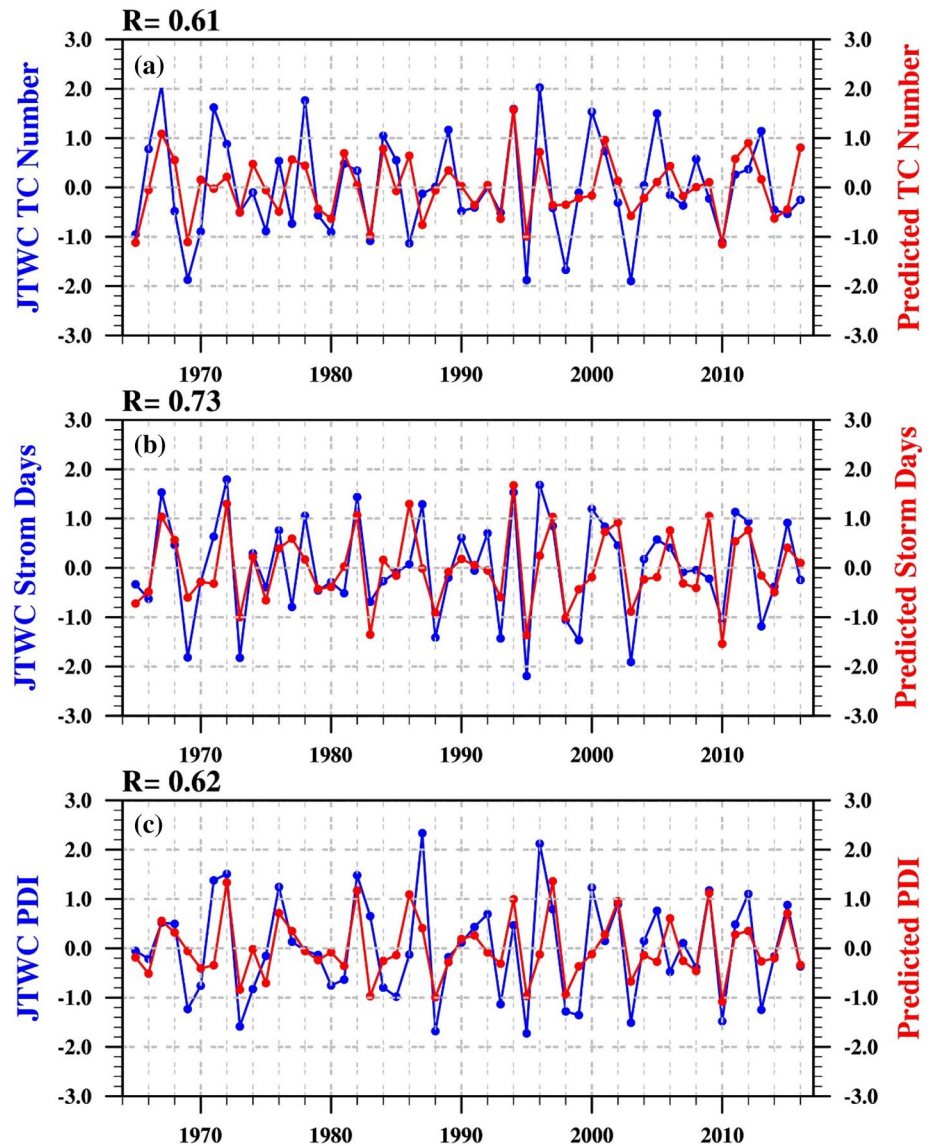

east of 120°E (Wang et al. 2010), and the PDI is defined as the cubic power of the 96-h maximum wind speed summed along the TC lifetime over the WNP (Emanuel 2005). It can be seen that about 40% of the total variance of TC activity can be reproduced by the simulation, suggesting that to a considerable extent, the TC activity variability can be predicted if dynamic models can perfectly forecast the two WNPSH modes. This provides a practical estimate for the lower bound of the WNPSH-related potential predictability for TC activity over the WNP.

The WNPSH-related TC potential predictability lends confidence to predict the TC activity by constructing PEMs with the predicted two WNPSH modes as predictors. Indeed, the results display valuable predicting skills (Fig. 12). The predicted (simulated) TC genesis frequency, tropical storm days and the PDI over the WNP can achieve significant TCC

skills of 0.59, 0.6 and 0.6 during 1965–2016, respectively. It should be noted that the predictability source of WNP TC genesis frequency mainly comes from the second mode of WNPSH, while the first mode has little contribution (Fig. 7). Additionally, the cross-validated reforecast and independent forecast reasonably reproduced interannual variation of the TC metrics as well. For the TC genesis number, the TCC (MSSS) skill of cross-validated reforecast during 1965–2000 is 0.55 (0.17), and the independent forecast has significant TCC skill of 0.56 for the recent 16 years (2001–2016). The TCC skills of the cross-validated reforecast and independent forecast for the tropical storm days (PDI) are 0.59 (0.46) and 0.52 (0.71), respectively.

Fig. 12 Prediction skills of the PEMs for the TC activity over the WNP. Time series of **a** TC genesis number, **b** tropical storm days and PDI obtained from the JTWC best track (black line), cross validated reforecast (blue line) and prediction (green line). The corresponding TCC and MSSS are shown in the bottom of each panel
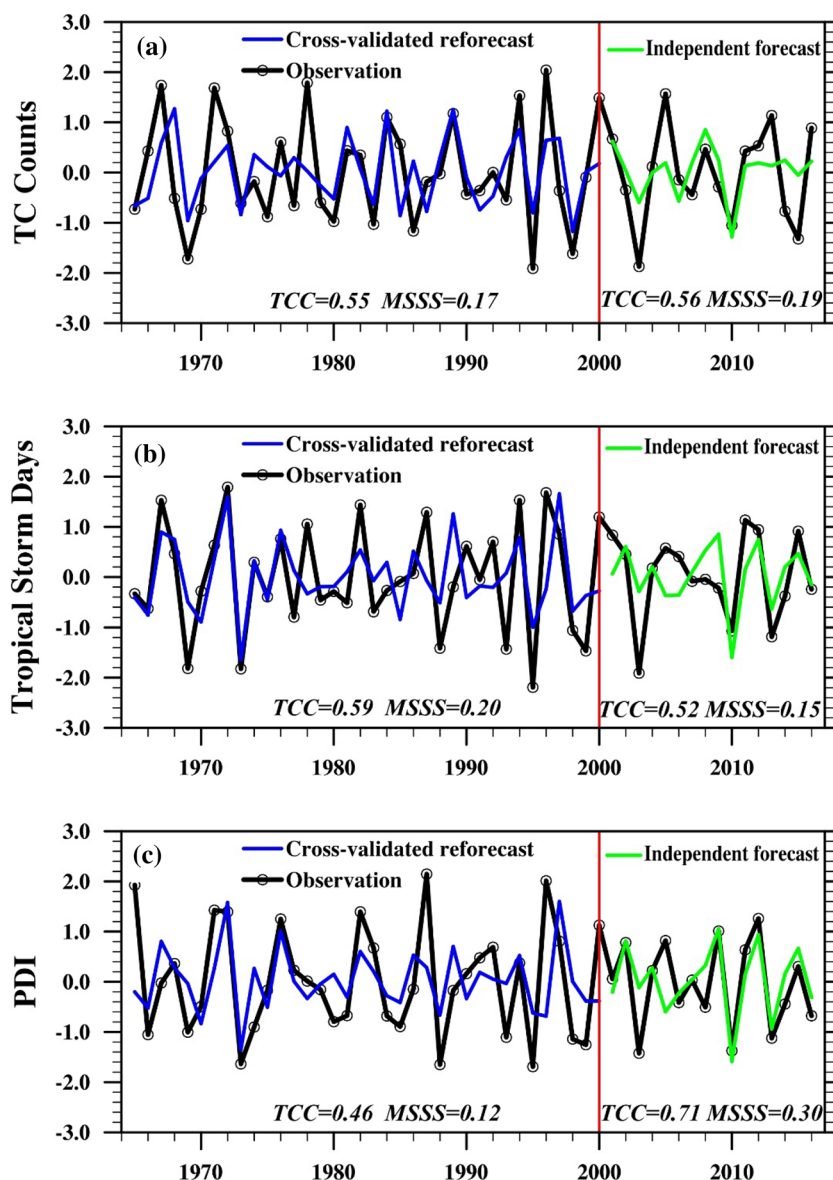
6 Summary

6.1 Conclusion

We find that the two leading EOF modes of WNPSH can integrate the effects of the trans-basin SST anomalies in the Pacific, Atlantic and Indian oceans on TC activity, and thus establish a unified framework to understand the inter-annual variability of the TC genesis, track and intensity. Particularly, the first mode, which shows an anti-cyclonic circulation anomaly occupying the entire WNP with two centers located at (18°N, 150°E) and the northern South China Sea, can integrate the effects of ENSO and Atlantic SST variations. The second mode is a coupled atmosphere–ocean mode between the anomalous WNPSH and underlying

Indo-Pacific warm pool, which can incorporate the Indian ocean SST effects.

It is shown that the first mode has insignificant influences on the total TC genesis frequency but can shift locations of TC formation southeastward or northwestward. However, the second mode is significantly correlated with the total TC genesis number. All of these variations are found to be consistent with large-scale conditions associated with the GPI.

A set of PEMs is built to predict the two WNPSH modes in the TC peak season (July–September) with May–June mean trans-basin SST predictors. The PEMs can reproduce very well the inter-annual variability of the two WNPSH modes and reasonably well the TC activity. In particular, the cross-validated reforecast (independent forecast) of the first mode for 1965–2000 (2001–2016)

achieves significant TCC skill of 0.79 (0.83). For the second mode, the cross-validated reforecast and independent forecast can achieve significant TCC skill of 0.73 and 0.56, respectively. Taking the predicted two WNPSH modes as predictors, we further established a set of PEMs to predict the TC genesis number, tropical storm days and PDI in July–September. The cross-validated reforecast (independent forecast) for genesis number, tropical storm days and PDI for 1965–2000 (2001–2016) achieves significant TCC skill of 0.55 (0.56), 0.59 (0.52), 0.46 (0.71), respectively. Considering the coupled models remain to be difficult to resolve TCs (Camargo 2013; Tory et al. 2013; Davis 2018), the significant prediction skills here have important application to the seasonal forecasting of TC activity over the WNP.

6.2 Discussion

Although the prediction skills for the TC metrics are statistically significant, one may note that only 20–30% of the total variance can be predicted by using the current prediction schemes. Such a limited predicting skill may partially result from the inadequate targeted predictands for the whole WNP, because previous studies have found that the TC activity over the WNP experiences distinct regional features, and this might make it difficult to predict the TC activity over the WNP as a whole (Wang and Chan 2002; Kim et al. 2010). Therefore, we further predicted TC genesis frequency in five sub-regions [i.e., South China Sea (0°–30°N, 100°E–120°E), southwest WNP (0°–16°N, 120°E–140°E), northwest WNP (16°N–40°N, 120°E–140°E), southeast WNP (0°–16°N, 140°E–180°) and northwest WNP (16°N-40°N,140°E-180°)]. It is found that the predictability comes mainly from the east and northwest WNP, while the prediction skills in the South China Sea and southwest WNP are relatively low. Such a low predictability in the two sub-regions limits the predicting skill.

In addition, we also try to forecast the TC genesis frequency in the five sub-region forecasts by using the four WNPSH predictors (SST anomalies) directly, and the results are generally similar to those by taking the predicted two WNPSH modes as predictors. These results suggest that the potential predictors may vary from one sub-region to another due to distinct regional features of climatological large-scale parameters over the WNP (Wang and Chan 2002; Camargo et al. 2007b; Tippett et al. 2011). Therefore, Consideration of TC prediction in individual sub-regions of the vast WNP with different predictors may be a more viable strategy, and we intend to explore this issue in a future study.

References

Camargo SJ (2013) Global and regional aspects of tropical cyclone activity in the CMIP5 models. J Clim 26:9880–9902. https://doi.org/10.1175/JCLI-D-12-00549.1

Camargo SJ, Sobel AH (2005) Western North Pacific tropical cyclone intensity and ENSO. J Clim 18:2996–3006. https://doi.org/10.1175/JCLI3457.1

Camargo SJ, Barnston AG, Klotzbach PJ, Landsea CW (2007a) Seasonal tropical cyclone forecasts. WMO Bull 56:297–309

Camargo SJ, Emanuel KA, Sobel AH (2007b) Use of a genesis potential index to diagnose ENSO effects on tropical cyclone genesis. J Clim 20:4819–4834. https://doi.org/10.1175/JCLI4282.1

Camp J, Roberts M, Maclachlan C, Wallace E, Hermanson L, Brookshaw A, Arribas A, Scaife AA (2015) Seasonal forecasting of tropical storms using the Met Office GloSea5 seasonal forecast system. Q J R Meteorol Soc 141:2206–2219. https://doi.org/10.1002/qj.2516

Chan JCL (1985) Tropical cyclone activity in the northwest Pacific in relation to the El Niño/Southern Oscillation phenomenon. Mon Weather Rev 113:599–606

Chan JCL (2000) Tropical cyclone activity over the western North Pacific associated with El Niño and La Niña events. J Clim 13:2960–2972. https://doi.org/10.1175/1520-0442(2000)013%3C2960:TCAOTW%3E2.0.CO;2

Chan JCL (2005) Interannual and interdecadal variations of tropical cyclone activity over the western North Pacific. Meteorol Atmos Phys 89:143–152. https://doi.org/10.1007/s00703-005-0126-y

Chan JC (2006) Comment on "Changes in tropical cyclone number, duration, and intensity in a warming environment". Science (80–) 311:1713. https://doi.org/10.1126/science.1121522 **(author reply 1713)**

Chan JCL, Shi JJ (1996) Long-term trends and interannual variability in tropical cyclone activity over the western North Pacific. Geophys Res Lett 23:2765–2767. https://doi.org/10.1029/96gl02637

Chan JCL, Shi JJ, Lam C-M. 1998: Seasonal forecasting of tropical cyclone activity over theWestern North Pacific and the South China Sea. Weather Forecast 13:997–1004. https://doi.org/10.1175/1520-0434(1998)013%3C0997:SFOTCA%3E2.0.CO;2

Chan JCL, Shi J-E, Liu KS 2001: Improvements in the seasonal forecasting of tropical cyclone activity over the Western North Pacific. Weather Forecast 16:491–498. https://doi.org/10.1175/1520-0434(2001)016%3C0491:IITSFO%3E2.0.CO;2

Chen J-H, Lin S-J (2013) seasonal predictions of tropical cyclones using a 25-km-resolution general circulation model. J Clim 26:380–398. https://doi.org/10.1175/JCLI-D-12-00061.1

Chen T-C, Weng S-P, Yamazaki N, Kiehne S (1998) Interannual variation in the tropical cyclone formation over the western North Pacific. Mon Weather Rev 126:1080–1090

Chen T-C, Wang S-Y, Yen M-C (2006) Interannual variation of the tropical cyclone activity over the western North Pacific. J Clim 19:5709–5720

Chia HH, Ropelewski CF (2002) The interannual variability in the genesis location of tropical cyclones in the northwest Pacific. J Clim 15:2934–2944

Chiang JCH, Vimont DJ (2004) Analogous Pacific and Atlantic meridional modes of tropical atmosphere–ocean variability. J Clim 17:4143–4158. https://doi.org/10.1175/JCLI4953.1

Chung P-H, Sui C-H, Li T (2011) Interannual relationships between the tropical sea surface temperature and summertime subtropical anticyclone over the western North Pacific. J Geophys Res. https://doi.org/10.1029/2010jd015554

Davis CA (2018) Resolving tropical cyclone intensity in models. Geophys Res Lett. https://doi.org/10.1002/2017GL076966

Du Y, Xie SP, Huang G, Hu K (2009) Role of air-sea interaction in the long persistence of El Niño-induced north Indian Ocean warming. J Clim 22:2023–2038. https://doi.org/10.1175/2008JCLI2590.1

Du Y, Yang L, Xie S-P (2011) Tropical Indian Ocean influence on Northwest Pacific tropical cyclones in summer following strong El Niño*. J Clim 24:315–322. https://doi.org/10.1175/2010JCLI3890.1

Emanuel K (2005) Increasing destructiveness of tropical cyclones over the past 30 years. Nature 436:686–688. https://doi.org/10.1038/nature03906

Emanuel KA, Nolan DS (2004) Tropical cyclone activity and the global climate system. Preprints. 26th conference on hurricanes and tropical meteorology, Miami, FL, Amer. Meteor. Soc. A, vol. 10 of

Fan K, Wang H (2009) A new approach to forecasting typhoon frequency over the Western North Pacific. Weather Forecast 24:974–986. https://doi.org/10.1175/2009WAF2222194.1

Gray WM (1968) Global view of the origin of tropical disturbances and storms. Mon Weather Rev 96:669–700

Ham Y-G, Kug J-S, Park J-Y, Jin F-F (2013) Sea surface temperature in the north tropical Atlantic as a trigger for El Niño/Southern Oscillation events. Nat Geosci 6:112–116. https://doi.org/10.1038/ngeo1686

He C, Zhou T (2014) The two interannual variability modes of the Western North Pacific subtropical high simulated by 28 CMIP5–AMIP models. Clim Dyn 43:2455–2469. https://doi.org/10.1007/s00382-014-2068-x

Ho C-H, Baik J-J, Kim J-H, Gong D-Y, Sui C-H (2004) Interdecadal changes in summertime typhoon tracks. J Clim 17:1767–1776

Huang B et al (2015) Extended reconstructed sea surface temperature version 4 (ERSST.v4). Part I: upgrades and intercomparisons. J Clim 28:911–930. https://doi.org/10.1175/JCLI-D-14-00006.1

Huangfu J, Huang R, Chen W, Feng T, Wu L (2017) Interdecadal variation of tropical cyclone genesis and its relationship to the monsoon trough over the western North Pacific. Int J Climatol 37:3587–3596. https://doi.org/10.1002/joc.4939

Huo L, Guo P, Hameed SN, Jin D (2015) The role of tropical Atlantic SST anomalies in modulating western North Pacific tropical cyclone genesis. Geophys Res Lett 42:2378–2384. https://doi.org/10.1002/2015GL063184

Kajtar JB, Santoso A, McGregor S, England MH, Baillie Z (2017) Model under-representation of decadal Pacific trade wind trends and its link to tropical Atlantic bias. Clim Dyn 0:1–14. https://doi.org/10.1007/s00382-017-3699-5

Kalnay E et al (1996) The NCEP/NCAR 40-year reanalysis project. Bull Am Meteorol Soc 77:437–471

Kim J-H, Ho C-H, Chu P-S (2010) Dipolar redistribution of summertime tropical cyclone genesis between the Philippine Sea and the northern South China Sea and its possible mechanisms. J Geophys Res. https://doi.org/10.1029/2009jd012196

Kim H-M, Webster PJ, Curry JA (2011) Modulation of North Pacific tropical cyclone activity by three phases of ENSO. J Clim 24:1839–1849. https://doi.org/10.1175/2010JCLI3939.1

Kim O-Y, Kim H-M, Lee M-I, Min Y-M (2017) Dynamical–statistical seasonal prediction for western North Pacific typhoons based on APCC multi-models. Clim Dyn 48:71–88. https://doi.org/10.1007/s00382-016-3063-1

Kucharski F, Kang I-S, Farneti R, Feudale L (2011) Tropical Pacific response to 20th century Atlantic warming. Geophys Res Lett. https://doi.org/10.1029/2010GL046248

Lander MA (1993) Comments on "A GCM simulation of the relationship between tropical storm formation and ENSO". Mon Weather Rev 121:2137–2143. https://doi.org/10.1175/1520-0493(1993)121%3C2137:COGSOT%3E2.0.CO;2

Lander MA (1994) An exploratory analysis of the relationship between tropical storm formation in the Western North Pacific and ENSO. Mon Weather Rev 122:636–651. https://doi.org/10.1175/1520-0493(1994)122%3C0636:AEAOTR%3E2.0.CO;2

Lau N-C, Nath MJ (2003) Atmosphere–ocean variations in the Indo-Pacific sector during ENSO episodes. J Clim. https://doi.org/10.1175/1520-0442%282003%29016%3C0003%3AAOVITI%3E2.0.CO%3B2

Lau N-C, Nath MJ, Wang H (2004) Simulations by a GFDL-GCM of ENSO related variability of the coupled atmosphere-ocean system in the East Asia monsoon region. In: Chang CP (ed) East Asian Monsoon. World Scientific, Singapore, pp 271–300. https://doi.org/10.1142/9789812701411_0007

Li J, Wang B (2017) Predictability of summer extreme precipitation days over eastern China. Clim Dyn 1:1–12. https://doi.org/10.1007/s00382-017-3848-x

Li X, Xie S-P, Gille ST, Yoo C (2015) Atlantic-induced pan-tropical climate change over the past three decades. Nat Clim Change 6:275–279. https://doi.org/10.1038/nclimate2840

Li T, Wang B, Wu B, Zhou T, Chang C, Zhang R (2017) Theories on formation of an anomalous anticyclone in western North Pacific during El Niño: a review. J Meteorol Res 31:987–1006. https://doi.org/10.1007/s13351-017-7147-6

Liu KS, Chan JCL (2008) Interdecadal variability of Western North Pacific tropical cyclone tracks. J Clim 21:4464–4476. https://doi.org/10.1175/2008jcli2207.1

Liu KS, Chan JCL (2013) Inactive period of Western North Pacific tropical cyclone activity in 1998–2011. J Clim 26:2614–2630. https://doi.org/10.1175/JCLI-D-12-00053.1

Lu M-M, Chu P-S, Lin Y-C (2010) Seasonal prediction of tropical cyclone activity near Taiwan using the Bayesian multivariate regression method. Weather Forecast 25:1780–1795. https://doi.org/10.1175/2010WAF2222408.1

Luo X, Wang B (2017) How predictable is the winter extremely cold days over temperate East Asia? Clim Dyn 48:2557–2568. https://doi.org/10.1007/s00382-016-3222-4

Manganello JV et al (2016) Seasonal forecasts of tropical cyclone activity in a high-atmospheric-resolution coupled prediction system. J Clim 29:1179–1200. https://doi.org/10.1175/JCLI-D-15-0531.1

Matsuura T, Yumoto M, Iizuka S (2003) A mechanism of interdecadal variability of tropical cyclone activity over the western North Pacific. Clim Dyn 21:105–117. https://doi.org/10.1007/s00382-003-0327-3

McGregor S, Timmermann A, Stuecker MF, England MH, Merrifield M, Jin FF, Chikamoto Y (2014) Recent walker circulation strengthening and pacific cooling amplified by atlantic warming. Nat Clim Change 4:888–892. https://doi.org/10.1038/nclimate2330

Michaelsen J (1987) Cross-validation in statistical climate forecast models. J Clim Appl Meteorol 26:1589–1600. https://doi.org/10.1175/1520-0450(1987)026%3C1589:CVISCF%3E2.0.CO;2

Murakami H, Wang B (2010) Future change of North Atlantic tropical cyclone tracks: Projection by a 20-km-mesh global atmospheric

model. J Clim 23:2699–2721. https://doi.org/10.1175/2010J CLI3338.1

Murphy AH (1988) skill scores based on the mean square error and their relationships to the correlation coefficient. Mon Weather Rev 116:2417–2424. https://doi.org/10.1175/1520-0493(1988)116%3C2417:SSBOTM%3E2.0.CO;2

Park J-Y, Jhun J-G, Yim S-Y, Kim W-M (2010) Decadal changes in two types of the western North Pacific subtropical high in boreal summer associated with Asian summer monsoon/El Niño–Southern Oscillation connections. J Geophys Res. https://doi.org/10.1029/2009jd013642

Rasmusson EM, Carpenter TH (1982) Variations in tropical sea surface temperature and surface wind fields associated with the Southern Oscillation/El Niño. Mon Weather Rev 110:354–384

Stuecker MF, Timmermann A, Jin F-F, McGregor S, Ren H-L (2013) A combination mode of the annual cycle and the El Niño/Southern Oscillation. Nat Geosci 6:540–544. https://doi.org/10.1038/ngeo1826

Stuecker MF, Jin F-F, Timmermann A, McGregor S (2015) Combination mode dynamics of the anomalous Northwest Pacific Anticyclone*. J Clim 28:1093–1111. https://doi.org/10.1175/JCLI-D-14-00225.1

Sui C-H, Chung P-H, Li T (2007) Interannual and interdecadal variability of the summertime western North Pacific subtropical high. Geophys Res Lett. https://doi.org/10.1029/2006gl029204

Tao L, Wu L, Wang Y, Yang J (2012) Influence of tropical Indian Ocean Warming and ENSO on tropical cyclone activity over the Western North Pacific. J Meteorol Soc Jpn 90:127–144. https://doi.org/10.2151/jmsj.2012-107

Tippett MK, Camargo SJ, Sobel AH (2011) A Poisson regression index for tropical cyclone genesis and the role of large-scale vorticity in genesis. J Clim 24:2335–2357. https://doi.org/10.1175/2010jcli3811.1

Tory KJ, Chand SS, McBride JL, Ye H, Dare RA (2013) Projected changes in late-twenty-first-century tropical cyclone frequency in 13 coupled climate models from phase 5 of the coupled model intercomparison project. J Clim 26:9946–9959. https://doi.org/10.1175/jcli-d-13-00010.1

Vecchi GA, Soden BJ (2007) Effect of remote sea surface temperature change on tropical cyclone potential intensity. Nature 450:1066–1070. https://doi.org/10.1038/nature06423

Vecchi GA et al (2014) On the seasonal forecasting of regional tropical cyclone activity. J Clim 27:7994–8016. https://doi.org/10.1175/JCLI-D-14-00158.1

Vimont DJ, Battisti DS, Hirst AC (2001) Footprinting: a seasonal connection between the tropics and mid-latitudes. Geophys Res Lett 28:3923–3926. https://doi.org/10.1029/2001GL013435

Wang B (1992) The vertical structure and development of the ENSO anomaly mode during 1979–1989. J Atmos Sci 49:698–712. https://doi.org/10.1175/1520-0469(1992)049%3C0698:TVSADO%3E2.0.CO;2

Wang, B, Chan JCL (2002) How strong ENSO events affect tropical storm activity over the western North Pacific. J Clim 15:1643–1658. https://doi.org/10.1175/1520-0442(2002)015%3C1643:HSEEAT%3E2.0.CO;2.

Wang C, Wu L (2012) Tropical cyclone intensity change in the Western North Pacific: downscaling from IPCC AR4 experiments. J Meteorol Soc Jpn 90:223–233. https://doi.org/10.2151/jmsj.2012-205. http://japanlinkcenter.org/DN/JST.JSTAGE/jmsj/2012-205?lang=en&from=CrossRef&type=abstract

Wang C, Wu L (2015) Influence of future tropical cyclone track changes on their basin-wide intensity over the western North Pacific: downscaled CMIP5 projections. Adv Atmos Sci 32:613–623. https://doi.org/10.1007/s00376-014-4105-4

Wang C, Wu L (2016) Interannual shift of the tropical upper-tropospheric trough and its influence on tropical cyclone formation over the Western North Pacific. J Clim 29:4203–4211. https://doi.org/10.1175/JCLI-D-15-0653.1

Wang C, Wu L (2018a) Projection of North Pacific tropical upper-tropospheric trough in CMIP5 models: implications for changes in tropical cyclone formation locations. J Clim 31:761–774. https://doi.org/10.1175/JCLI-D-17-0292.1

Wang C, Wu L (2018b) Future changes of the monsoon trough: sensitivity to sea surface temperature gradient and i***mplications for tropical cyclone activity. Earth's Future 6:919–936. https://doi.org/10.1029/2018EF000858

Wang B, Wu R, Fu X (2000) Pacific–East Asian teleconnection: how does ENSO affect East Asian Climate? J Clim 13:1517–1536. https://doi.org/10.1175/1520-0442(2000)013%3C1517:PEATHD%3E2.0.CO;2

Wang B, Wu R, Li TIM (2003) Atmosphere-warm ocean interaction and its impacts on Asian-Australian Monsoon Variation*. J Clim 16:1195–1211. https://doi.org/10.1175/1520-0442(2003)16%3C1195:AOIAII%3E2.0.CO;2

Wang B, Yang Y, Ding Q-H, Murakami H, Huang F (2010) Climate control of the global tropical storm days (1965–2008). Geophys Res Lett. https://doi.org/10.1029/2010GL042487

Wang B, Xiang B, Lee J-Y (2013a) Subtropical high predictability establishes a promising way for monsoon and tropical storm predictions. Proc Natl Acad Sci 110:2718–2722. https://doi.org/10.1073/pnas.1214626110

Wang C, Li C, Mu M, Duan W (2013b) Seasonal modulations of different impacts of two types of ENSO events on tropical cyclone activity in the western North Pacific. Clim Dyn 40:2887–2902. https://doi.org/10.1007/s00382-012-1434-9

Wang B, Xiang B, Li J, Webster PJ, Rajeevan MN, Liu J, Ha K-J (2015) Rethinking Indian monsoon rainfall prediction in the context of recent global warming. Nat Commun 6:7154. https://doi.org/10.1038/ncomms8154

Wang B, Li J, He Q (2017) Variable and robust East Asian monsoon rainfall response to El Niño over the past 60 years (1957–2016). Adv Atmos Sci 34:1235–1248. https://doi.org/10.1007/s00376-017-7016-3

Wang C, Wang B, Wu L (2018a) Abrupt breakdown of the predictability of early season typhoon frequency at the beginning of the twenty-first century. Clim Dyn. https://doi.org/10.1007/s00382-018-4350-9

Wang C, Wu L, Zhao H, Cao J, Tian W (2018b) Is there a quiescent typhoon season over the western North Pacific following a strong El Niño event? Int J Climatol. https://doi.org/10.1002/joc.5782

Wilks DS (2006) Statistical methods in the atmospheric sciences. Academic Press, p 676

Wing AA, Sobel AH, Camargo SJ (2007) Relationship between the potential and actual intensities of tropical cyclones on interannual time scales. Geophys Res Lett. https://doi.org/10.1029/2006gl028581

Wu L, Wang C (2015) Has the western pacific subtropical high extended westward since the late 1970s? J Clim 28:5406–5413. https://doi.org/10.1175/JCLI-D-14-00618.1

Wu LB, Wang, Geng S (2005) Growing typhoon influence on east Asia. Geophys Res Lett. https://doi.org/10.1029/2005GL022937

Wu B, Zhou T, Li T (2009) seasonally evolving dominant interannual variability modes of East Asian Climate*. J Clim 22:2992–3005. https://doi.org/10.1175/2008jcli2710.1

Wu L, Wen Z, Huang R, Wu R (2012) Possible linkage between the monsoon trough variability and the tropical cyclone activity over the Western North Pacific. Mon Weather Rev 140:140–150. https://doi.org/10.1175/MWR-D-11-00078.1

Wu L, Wang C, Wang B (2015) Westward shift of western North Pacific tropical cyclogenesis. Geophys Res Lett 42:1537–1542. https://doi.org/10.1002/2015GL063450

Wu Y-K, Hong C-C, Chen C-T (2018) Distinct effects of the two strong El Niño events in 2015–2016 and 1997–1998 on the Western North Pacific monsoon and tropical cyclone activity: role of subtropical eastern North Pacific Warm SSTA. J Geophys Res Ocean 123:3603–3618. https://doi.org/10.1002/2018JC013798

Xiang B, Wang B, Yu W, Xu S (2013) How can anomalous western North Pacific Subtropical High intensify in late summer? Geophys Res Lett 40:2349–2354. https://doi.org/10.1002/grl.50431

Xie S-P, Hu K, Hafner J, Tokinaga H, Du Y, Huang G, Sampe T (2009) Indian ocean capacitor effect on Indo–Western Pacific climate during the summer following El Niño. J Clim 22:730–747. https://doi.org/10.1175/2008JCLI2544.1

Xie S-P, Kosaka Y, Du Y, Hu K, Chowdary JS, Huang G (2016) Indo-western Pacific ocean capacitor and coherent climate anomalies in post-ENSO summer: a review. Adv Atmos Sci 33:411–432. https://doi.org/10.1007/s00376-015-5192-6

Yang J, Liu Q, Xie S-P, Liu Z, Wu L (2007) Impact of the Indian Ocean SST basin mode on the Asian summer monsoon. Geophys Res Lett. https://doi.org/10.1029/2006gl028571

Yu J, Li T, Tan Z, Zhu Z (2015) Effects of tropical North Atlantic SST on tropical cyclone genesis in the western North Pacific. Clim Dyn. https://doi.org/10.1007/s00382-015-2618-x

Zhan R, Wang Y (2016) CFSv2-based statistical prediction for seasonal accumulated cyclone energy (ACE) over the western North Pacific. J Clim 29:525–541. https://doi.org/10.1175/JCLI-D-15-0059.1

Zhan R, Wang Y, Lei X (2011) Contributions of ENSO and East Indian Ocean SSTA to the interannual variability of Northwest Pacific Tropical cyclone frequency. J Clim 24:509–521. https://doi.org/10.1175/2010JCLI3808.1

Zhan R, Wang Y, Ying M (2012) Seasonal forecasts of tropical cyclone activity over the western North Pacific: a review. Trop Cyclone Res Rev 1:307–324

Zhan R, Wang Y, Liu Q (2017) Salient differences in tropical cyclone activity over the Western North Pacific between 1998 and 2016. J Clim 30:9979–9997. https://doi.org/10.1175/JCLI-D-17-0263.1

Zhang Q, Wu L, Liu Q (2009) Tropical cyclone damages in China 1983–2006. Bull Am Meteorol Soc 90:489–495. https://doi.org/10.1175/2008BAMS2631.1

Zhang W, Vecchi GA, Murakami H, Villarini G, Jia L (2016a) The Pacific meridional mode and the occurrence of tropical cyclones in the Western North Pacific. J Clim 29:381–398. https://doi.org/10.1175/JCLI-D-15-0282.1

Zhang W, Villarini G, Vecchi GA, Murakami H, Gudgel R (2016b) Statistical-dynamical seasonal forecast of western North Pacific and East Asia landfalling tropical cyclones using the high-resolution GFDL FLOR coupled model. J Adv Model Earth Syst 8:538–565. https://doi.org/10.1002/2015MS000607

Zhang W, Vecchi GA, Villarini G, Murakami H, Rosati A, Yang X, Jia L, Zeng F (2017) Modulation of western North Pacific tropical cyclone activity by the Atlantic Meridional Mode. Clim Dyn 48:631–647. https://doi.org/10.1007/s00382-016-3099-2

Zhang W, Vecchi GA, Murakami H, Villarini G, Delworth TL, Yang X, Jia L (2018) Dominant role of Atlantic Multidecadal oscillation in the recent decadal changes in Western North Pacific tropical cyclone activity. Geophys Res Lett. https://doi.org/10.1002/2017GL076397

Zhao H, Wu L, Zhou W (2010) Assessing the influence of the ENSO on tropical cyclone prevailing tracks in the western North Pacific. Adv Atmos Sci 27:1361–1371. https://doi.org/10.1007/s00376-010-9161-9

Zhao H, Wu L, Zhou W (2011) Interannual changes of tropical cyclone intensity in the Western North Pacific. J Meteorol Soc Jpn 89:243–253. https://doi.org/10.2151/jmsj.2011-305